Bio-Medical Materials and Engineering 19 (2009) 11–17
DOI 10.3233/BME-2009-0558

Multiwalled Carbon Nanotube Monoliths prepared by Spark Plasma Sintering (SPS) and their Mechanical Properties

Motohiro Uo[1], Tomoka Hasegawa[1], Tsukasa Akasaka[1], Isao Tanaka[2], Fuminori Munekane[3], Mamoru Omori[4], Hisamichi Kimura[4], Reiko Nakatomi[5], Kohei Soga[5], Yasuo Kogo[5] and Fumio Watari[1]

[1]Department of Biomedical Materials and Engineering, Graduate School of Dental Medicine, Hokkaido University, Sapporo, JAPAN

[2]Shimizu Corporation, Tokyo, JAPAN

[3]Nano Carbon Technologies Co., Ltd, Tokyo, JAPAN

[4]Institute of Materials Research, Tohoku University, Sendai, JAPAN

[5]Department of Materials Science and Technology, Faculty of Industrial Science and Technology, Tokyo University of Science

Abstract

Three types of multiwalled carbon nanotube (MWCNT) monoliths without any binders were obtained by spark plasma sintering (SPS) treatment at 2000°C under 80MPa sintering pressure. Three MWCNTs with different diameters: thin (20~30nmϕ, CNT Co., Ltd., Korea), thick (100nmϕ, Nano Carbon Technologies Co., Ltd., Japan) and spherical thin (20~30nmϕ, granulated diameter=1~3μm, Shimizu Corporation, Japan)) were employed for SPS. SEM observation confirmed that these materials maintained the nanosized tube microstructure of raw CNT powder after SPS treatment. The densest monolith was prepared with the spherical MWCNTs. The mechanical properties of this material were estimated by the dynamic hardness test. The elastic modulus of the monolith did not depend on the difference of MWCNTs, but the hardness of spherical MWCNTs was higher than that of thick MWCNTs. The high density and hardness of the spherical MWCNTs were caused by the high packing density during the SPS process because of its spherical granulation. Thus, the spherical MWCNTs were most useful for the MWCNT monolith preparation with the SPS process and its application as a bone substitute material and a bone tissue engineering scaffold material was suggested.

1. Introduction

Carbon fiber-reinforced material shows high mechanical strength with light weight and it is widely employed in engineering and biomaterial applications[1-4]. Carbon nanotubes (CNTs) are similar to carbon fibers, but are smaller, with diameters in the tens of nanometers. CNTs have excellent mechanical properties compared to conventional carbon fibers, with low specific weight and high porosity compared to graphite because of their tubular structure[5-8]. Therefore, the bulk material of CNTs might be a good medical implant material for artificial bones and joints. On the other hand, the spark plasma sintering (SPS) method is well known as a suitable method for solidification of various ceramics, composites and other materials that are difficult to sinter. During SPS, powder is pressed in a graphite die unidirectionally and pulsed DC current is applied through the die. The pulsed DC current causes electrical spark discharges among the powder's particles and quite fast sintering is achieved. Wang et al. reported the SPS sintering of multiwalled carbon nanotubes (MWCNTs) using polycarbosilane (PCS) as a binder[9]. PCS formed SiC during the SPS process, which resulted in an MWCNT/SiC monolith that showed good mechanical properties. Wang et al. also succeeded in the preparation of an MWCNT monolith without a binder using the SPS process[10]. Both MWCNT monoliths showed good new bone formation in bone implantation tests. The compression strength of the MWCNT monolith without a binder was lower than that with PCS as a binder.

In this study, various types of MWCNTs were sintered using the SPS method and MWCNT monoliths were prepared without a binder. The effects of the tube diameter and morphology of the MWCNTs on the mechanical properties and microstructures of those MWCNT monoliths were estimated.

2. Experimental Procedure

2-1 Materials

The three different types of MWCNTs used in this study are presented in Table 1. Thin MWCNTs (20~30nmϕ in diameter, purity 80%), thick MWCNTs (100nmϕ in diameter) and spherical MWCNTs (20~30nmϕ in tube diameter and 1~3μmϕ in granule diameter) were employed for sintering. SEM images of each type of MWCNT are shown in Fig. 1. To purify them, thin MWCNTs were oxidized in air at 500^{o}C for 90 minutes and rinsed with 6M HCl aq., then washed with distilled water and dried. The CNT100 used in this study was supplied before the annealing process, which improved the crystalinity.

2-2 SPS sintering of MWCNTs

The graphite mold was filled with 0.2g of MWCNTs in (10mm in inner diameter) and sintered in an SPS (Dr. Sinter, Sumitomo Coal Mining, Japan) under 80MPa pressure at 2000^{o}C for 10min. The MWCNT monolith obtained was polished and subjected to SEM observation (S-4000, Hitachi, Japan) and the estimation of its mechanical properties. The specific surface areas (SSA) of MWCNT powders and sintered monoliths were estimated by the nitrogen absorption method (Flowsorp 3, Shimadzu, Japan).

2-3 Mechanical property estimation

The mechanical properties of the MWCNT monoliths were estimated by the dynamic hardness test (DUH-W201, Shimadzu, Japan). A typical load-displacement curve of this test is shown in Fig. 2. The elastic modulus of the MWCNT monolith was calculated using the following equations;

$A=(2Rh_p-h_p^2)^{0.5}$,

$S=2Er \cdot A^{0.5}/\pi^{0.5}$,

$1/Er=(1-\nu^2)/E+(1-\nu_i)/E_i$,

where Er= the complex elastic modulus of the specimen and probe,

E_i= the Young's modulus of the diamond probe ($1.14x10^{12}N/m^2$) s

A= the Elastic contact area, ν_i= Poisson's ratio of the probe(0.07),

R= the curvature of the indentor (30μm), E= the Elastic modulus of the specimen,

ν= the Poisson's ratio of the specimen (assumed to be 0.3), and

S,h_p= the slope and depth defined from the load-displacement curve shown in Fig. 2.

The dynamic hardness test in this study applied a spherical diamond probe (30μm) to the specimen surface until a constant load (100mN) was achieved. This method is similar to the Brinell hardness test. The Brinell hardness number (H_B) could be estimated with the following equation using the indentation depth which was given as "h_{max}" in Fig. 2.

$H_B = P / \pi R h_{max}$

where P = load (100mN), and h_{max} = depth of indentation.

3. Results

All MWCNTs were successfully sintered by SPS without binders at 2000°C for 40~80MPa. Figure 3 shows SEM images of SPS sintered into various MWCNT monoliths. Thin (CNT30) and spherical CNTs (Sp-CNT30) were densely packed after SPS and the tubular structure of MWCNTs was not damaged. Thick CNTs (CNT100) looked slightly porous. Mixed MWCNTs consisting of CNT30 (25wt%) and CNT100 (75wt%) were also sintered and had a microstructure similar to that of CNT100.

Table 2 shows the specific surface areas (SSA) of sintered MWCNT monoliths and MWCNT powders. The sintered CNT30 had the largest SSA ($57m^2/g$) and CNT100 had a small SSA ($15 m^2/g$). The sintered Sp-CNT30 had a low SSA ($22m^2/g$) in spite of the fact that the diameter of the nanotubes contained in Sp-CNT30 was similar to that of CNT30 (30nm). Thus, the dense sintering of Sp-CNT30 was also confirmed.

Figure 4 shows the elastic moduli estimated by the dynamic hardness test. There were no significant differences among CNT30, CNT100 and Sp-CNT30. Only the mixed MWCNT monolith (CNT30+100) had a smaller elastic modulus.

The Brinell hardness numbers estimated from the dynamic hardness testing of MWCNT monoliths are shown in Fig. 5. The Sp-CNT30 and CNT30 monoliths had higher hardness values than the monolith

consisting of CNT100. The Sp-CNT30 monolith had the highest Brinell hardness (H_B=55), with a smaller standard deviation than CNT30.

4. Discussion

SSA is an important parameter to estimate the porosity of sintered materials. The SSAs of all sintered MWCNTs were decreased from the powder state before sintering. The SSA of MWCNTs depended on their diameter, so thin MWCNTs (CNT30) had a larger SSA than thick MWCNTs (CNT100) and it was similar to that for spherical MWCNTs (Sp-CNT30), which had a similar tube diameter (~30nm). The low SSA of sintered CNT100 could be explained by the large tube diameter. However, the sintered Sp-CNT30 had a lower SSA than that of CNT30 even though their tube diameters were similar. This shows the denser sintering of Sp-CNT30 than for the other MWCNTs, which is also shown in the SEM images in Fig. 3.

To obtain the CNT monoliths, bonds among CNTs should be formed during SPS. Thin CNTs (CNT30) would contain many defects in their grapheme structure and be quite flexible. Thus, they were densely packed and sintered by SPS. In contrast, thick CNTs (CNT100) were less flexible and their graphene structure exhibited good crystalinity as show in Fig. 1. The CNT100 monolith became porous as shown in Fig. 3. Spherical CNTs (Sp-CNT30) were prepared with granulation treatment of thin MWCNTs. That provided high green density and good dispersibility in various solutions, and it was quite easy to handle compared to other MWCNTs without such treatment. Therefore, the sintered Sp-CNT30 had a low SSA and high mechanical strength compared to CNT30, even though they had similar tube diameters.

Concerning the mechanical properties, no significant change was observed in the elastic moduli of monoliths. However, the estimated Brinell hardness showed differences between thin MWCNTs (CNT30 and Sp-CNT30) and thick MWCNTs. The elastic modulus was evaluated from the slope of the load-displacement curve while unloading. Thus, the modulus reflects the elastic properties of dense MWCNTs and the high porosity of a thick MWCNT monolith would not affect the elastic modulus. The differences between the applied MWCNTs were only the outer diameter and shape of the aggregated granules. The atomic structures of graphene sheets of those MWCNTs are the same. Therefore the elastic moduli of those monoliths would not by affected by the difference of the tube diameter and shape of raw MWCNTs. The Sp-CNT30 monolith had the highest Brinell hardness (H_B=55) and the standard deviation of the hardness was smaller than that of the CNT30 monolith. This indicated that the Sp-CNT30 monolith was more homogeneously and densely sintered than CNT30. In contrast, the CNT100 monolith had low hardness, which was caused by the porous structure of the monolith as shown in Fig. 3. The commercial product of CNT100 could not be sintered by SPS even at 2000^{o}C and 80MPa because of its excellent structural stability. In this study, we succeeded in sintering by SPS using the intermediate product of CNT100 before annealing.

Kanari et al. evaluated the elastic moduli of a graphite and carbon/carbon (C/C) composite by a similar method[11]. The elastic moduli of a C/C composite were 1.97GPa for the matrix and 6.71GPa for the carbon fiber. Those values were lower than that of graphite (10.7GPa). The elastic moduli of MWCNT monoliths were between 3.5 and 4.6 GPa. These values were similar to that of the C/C composite and lower than for graphite. The C/C composite was prepared using carbonized 100μmϕ polyacrylonitrile fibers; thus, it had a micrometer-scale fibrous structure. The scale of the fibrous structure was quite different between the C/C composite and the MWCNT monoliths, but their elastic moduli were quite similar. Wang et al. reported good bone formation around an SPS sintered MWCNT monolith [9, 10]. They suggested that the mechanical properties of the MWCNT monolith were similar to natural bone, so it would be suitable as a bone substitute material.

In this study, a dense MWCNTs monolith could be prepared from spherical MWCNTs without a binder by using SPS. This would also be a candidate material for a bone substitute and a bone tissue engineering scaffold material.

Conclusions

MWCNT monoliths were prepared using SPS without binders. They were obtained by spark plasma sintering (SPS) treatment at 2000^{o}C under 80MPa sintering pressure. A dense monolith was obtained from spherical MWCNTs whose tube diameter was about 30nm. The elastic modulus of the monolith did not depend on the difference of MWCNTs, but the hardness of spherical MWCNTs was higher than that of thick MWCNTs. The high density and hardness of the spherical MWCNTs would be caused by the high packing density during the SPS process because of their spherical granulation. Thus, the spherical MWCNTs were most useful for MWCNT monolith preparation using the SPS process. The mechanical properties of the CNT monolith were suggested to be close to those of natural human bone. Therefore the MWCNT monolith could be a good bone substitute and bone tissue engineering scaffold material.

Acknowledgement

This work was supported by Research on Advanced Medical Technology in Health and Labour Sciences Research Grants from the Ministry of Health, Labour and Welfare of Japan.

References

[1] A.D. Haubold, H.S. Shim, J.C. Bokros, D.F. Williams (ed.), Biocompatibility of Clinical Implant Materials, Vol.2, p.3-42, CRC Press, Boca Raton, FL, 1981.

[2] D.J. Pemberton, B. McKibbin, R. Savage, K. Tayton, D. Stuart, Carbon-fibre reinforced plates for problem fractures, J. Bone Joint Surg. Br. 74 (1992) 88-92.

[3] L. Ma, G. Sines, Fatigue behavior of a pyrolytic carbon, J. Biomed. Mater. Res. 51 (2000) 61-68.

[4] K. Bitter, A.M. Kielbassa, Post-endodontic restorations with adhesively luted fiber-reinforced composite post systems: a review, Am. J. Dent. 20 (2007) 353-60.

[5] R.S. Ruoff, D.C. Lorents, Mechanical and thermal properties of carbon nanotubes, Carbon 33 (1995) 925-930.

[6] M.M.J. Treacy, T.W. Ebbesen, J.M. Gibson, Exceptionally high Young's modulus observed for individual carbon nanotubes, Nature 381 (1996) 678-679.

[7] J.P. Salvetat, G.A. Briggs, J.M. Bonard, R.R. Bacsa, A.J. Kulik, T. Stöckli, N.A. Burnham, L. Forró, Elastic and shear moduli of single-walled carbon nanotube ropes, Phys. Rev. Lett., 82 (1999) 944-947

[8] H. Miyagawa, M. Misra, A.K. Mohanty, Mechanical properties of carbon nanotubes and their polymer nanocomposites, J. Nanosci. Nanotechnol. 5 (2005) 1593-1615.

[9] W. Wang, F. Watari, M. Omori, S. Liao, Y. Zhu, A. Yokoyama, M. Uo, H. Kimura, A. Ohkubo**,** Mechanical properties and biological behavior of carbon nanotube/polycarbosilane composites for implant materials. J Biomed Mater Res B Appl Biomater, 82B (2007), 223-230

[10] W. Wang, A. Yokoyama, S. Liao, M. Omori, Y. Zhu, M. Uo, T. Akasaka, F. Watari, Preparation and characteristics of a binderless carbon nanotube monolith and its biocompatibility, Article in Press, Materials Science and Engineering C (2008) http://dx.doi.org/10.1016/j.msec.2007.04.038

[11] M. Kanari, K. Tanaka, S. Baba, M. Eto, Nanoindentation behavior of a two-dimensional carbon-carbon composite for nuclear applications, Carbon 25 (1997) 1429-1437.

Figure captions

Fig. 1 SEM images of MWCNTs used in this study.

Fig. 2 Typical load-displacement curve of the dynamic hardness test.

Fig. 3 SEM images of SPS sintered MWCNTs.

Fig. 4 Elastic moduli of SPS sintered MWCNT monoliths.

Fig. 5 Estimated Brinell hardness numbers of SPS sintered MWCNT monoliths.

Table 1 MWCNTs used in this study.

Abbreviation	Diameter (nm)	Specific surface area (m^2/g)	Manufacturer
CNT30	20~30	127	CNT Co., Ltd. (Korea)
CNT100	50~100	30	Nano Carbon Technologies Co., Ltd. (Japan)
Sp-CNT30	20~30	180	Shimizu Corporation

Table 2 Specific surface areas of sintered MWCNT monoliths.

MWCNT source	Specific surface area of sintered monolith (m^2/g)
CNT30	57
CNT100	15
CNT30+CNT100	37
Sp-CNT30	22

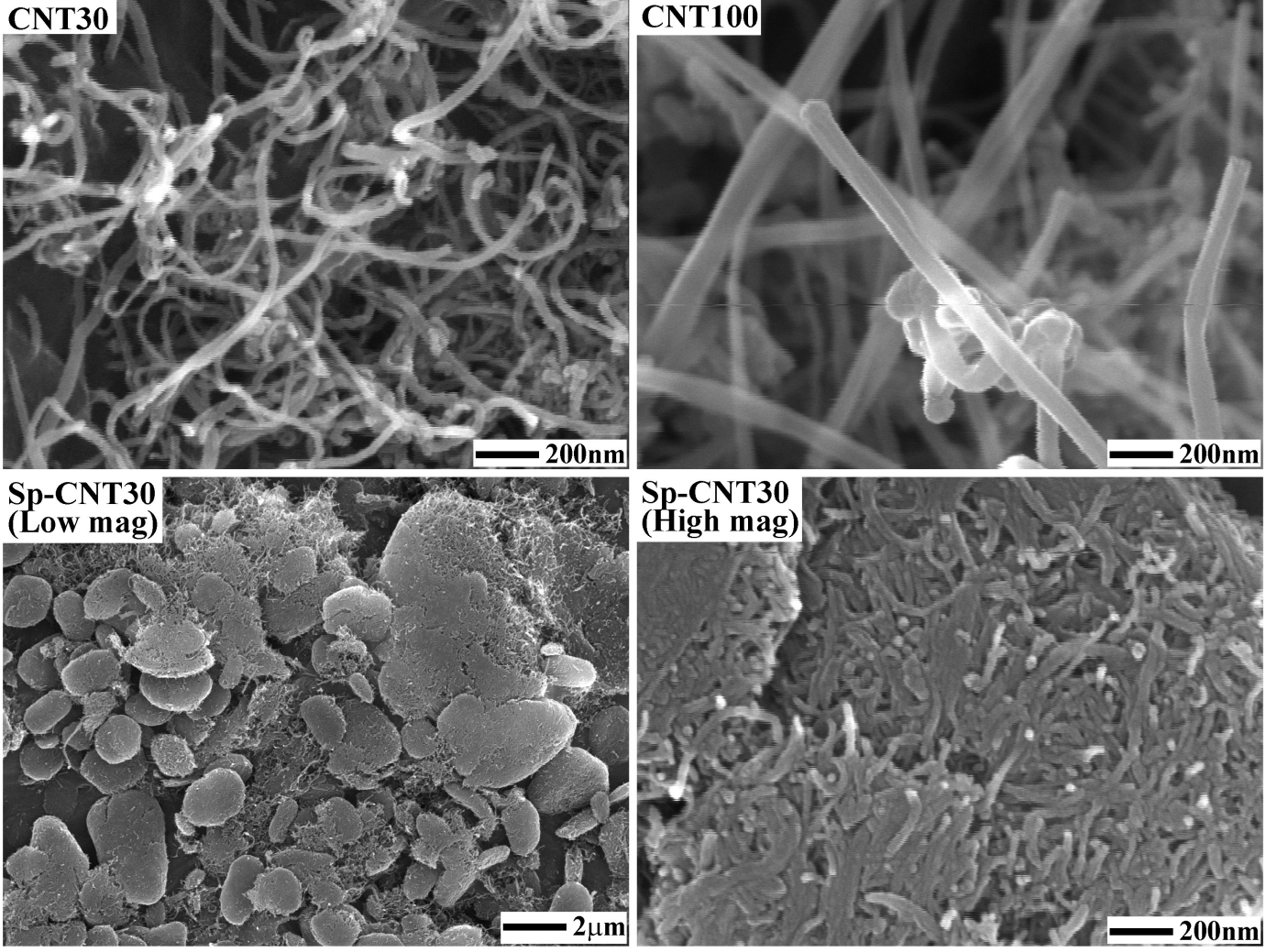
CNT30
200nm
CNT100
200nm
Sp-CNT30
(Low mag)
2μm
Sp-CNT30
(High mag)
200nm

Fig.1

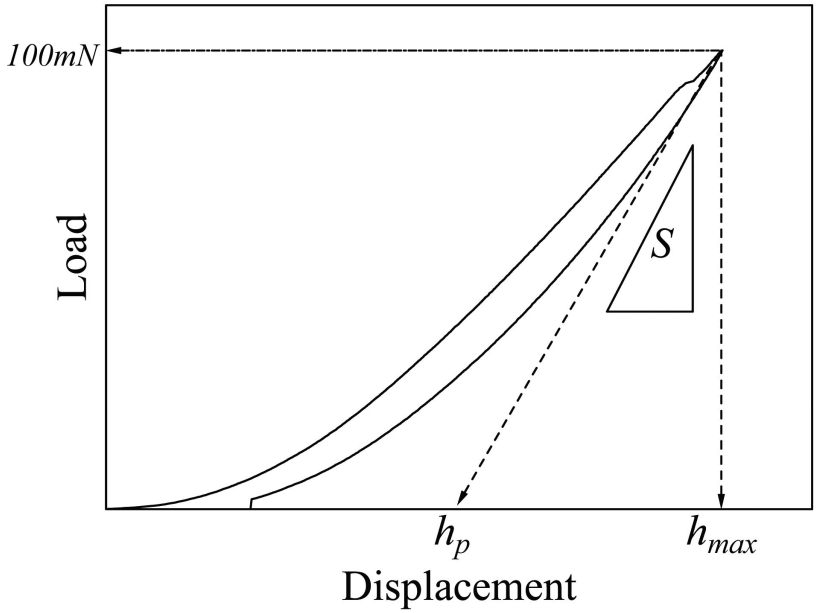
100mN
Load
S
h_p
h_{max}
Displacement

Fig.2

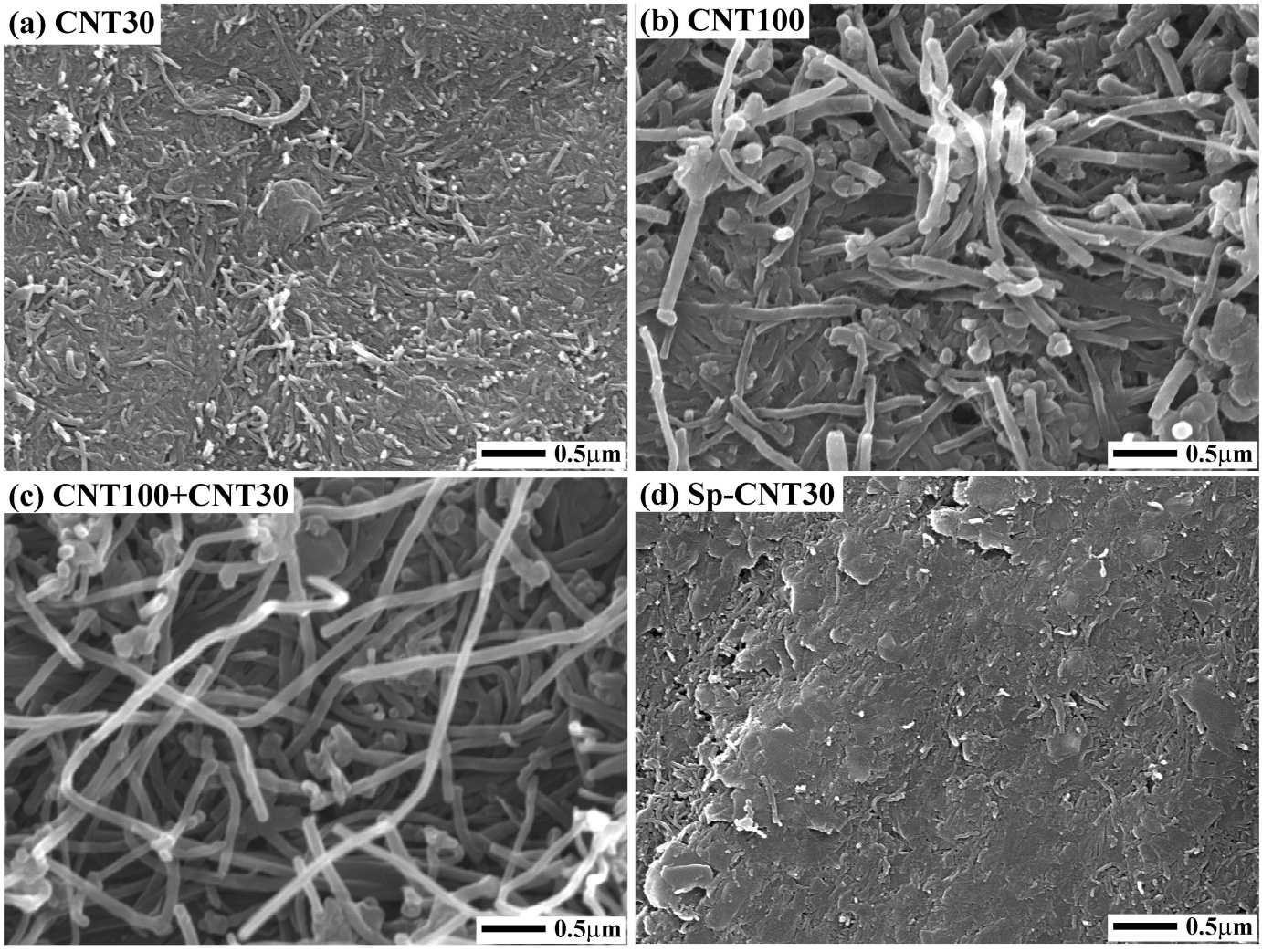

Fig.3

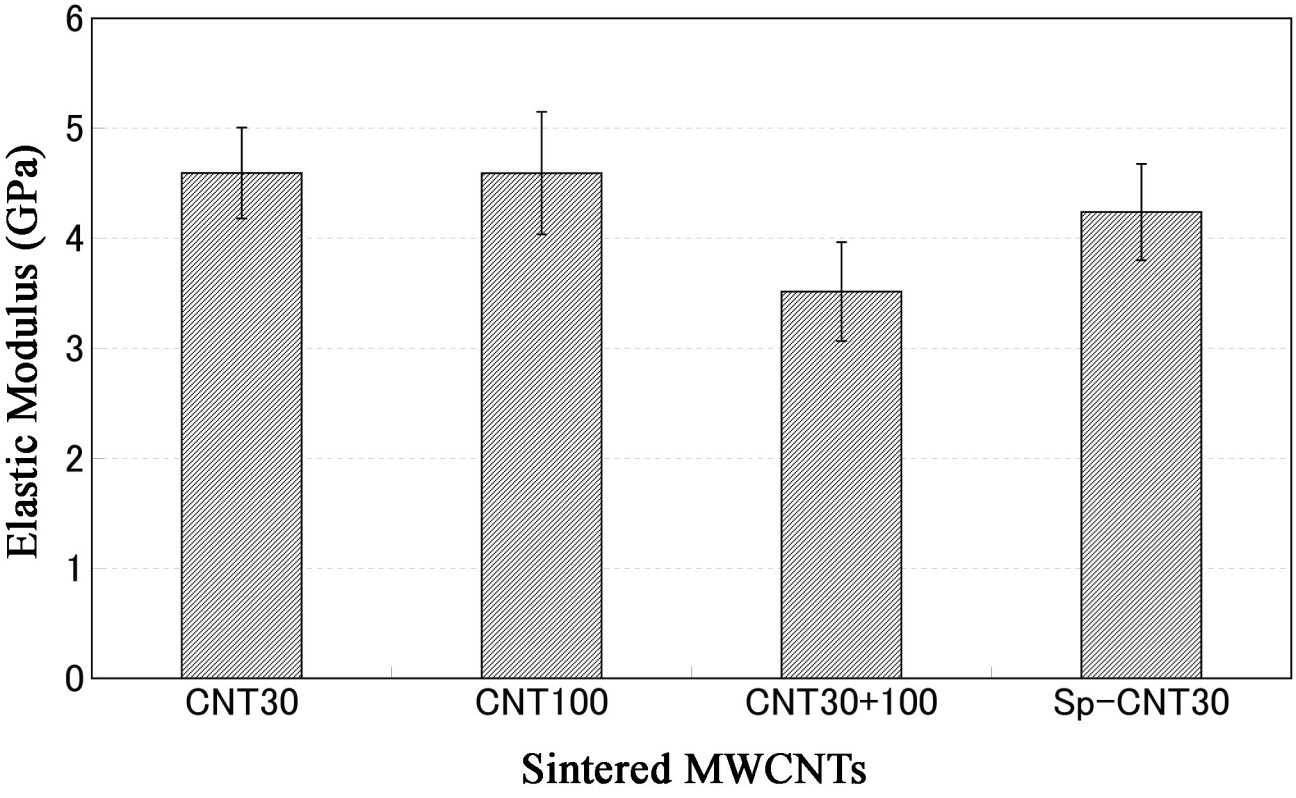
Elastic Modulus (GPa)
0
1
2
3
4
5
6
CNT30
CNT100
CNT30+100
Sp-CNT30
Sintered MWCNTs

Fig. 4

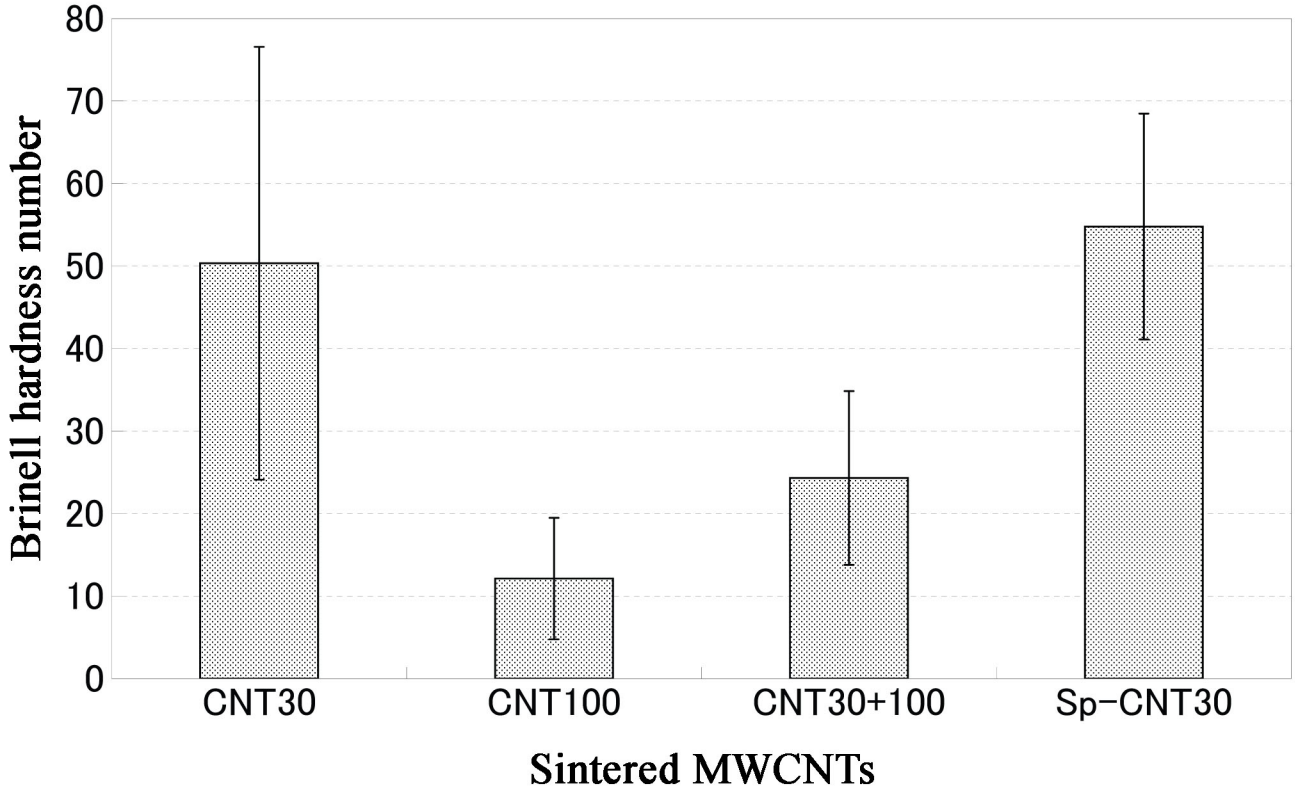
Brinell hardness number
0
10
20
30
40
50
60
70
80
CNT30
CNT100
CNT30+100
Sp-CNT30
Sintered MWCNTs

Fig.5